

Fully Variable Valve Control: A Geometric Approach

Anton Gfrerrer, Johann Lang

*Institute of Geometry, Graz University of Technology
Kopernikusgasse 24, 8010 Graz, Austria
email: gfrerrer@tugraz.at*

Abstract. Variable valve timing (VVT) and variable valve lift (VVL) are used to improve the performance, fuel economy and to reduce emissions of a combustion engine. Recently these issues have assumed increasing importance. Here we will combine VVT and VVL in a unified concept of *variable valve control* (VVC). We present a mechanical solution to fully variable valve control. The cam consists of two symmetric parts that slide on the camshaft; this way the system can provide a continuum of cam characteristics to meet a wide range of engine requirements.

Key Words: internal combustion engine, camshaft, valve timing, valve lift, valve control, surface interpolation, envelope surface

MSC 2010: 53A17, 53A04

1. Introduction

Early efforts in VVC in a combustion engine were made in the late 1950s and in the 1960s. Not before 1980, though, were the results applied in a production car. It was in the late 1980s when the first company (Honda) introduced some sort of variable valve control (VTEC) in a large scale [7]. Today each automobile manufacturer has his own approach to variable valve control. Their solutions are usually based on the concept of two different cam lobes being engaged depending on the rev range or on other parameters. Additionally, the whole camshaft can be twisted by a few degrees to allow earlier valve opening (and closing) which only affects VVT. One remarkable example of fully variable valve control is BMW's *Valvetronic system* [6, 8]. Two early review articles on VVT are [2] and [4], a more recent survey on VVC can be found in [3, pp. 185–193].

In this paper we introduce a geometric approach to fully variable valve control in a step-by-step procedure. The main idea is to construct a cam that is divided in two; its symmetric halves can be shifted along the camshaft axis such that their distance varies within a certain range while the plane of symmetry between them is fixed. Changing the distance between the two cam parts employs a continuum of lift profiles.

In Section 2 we start with a given series of lobe curves establishing the input data for our procedure. In Section 3 we create some virtual profile surface whose parameter lines represent an infinite set of lobe curves. In Section 4 we introduce the suggested cam mechanism and analyze its kinematics. The cam shape is characterized as the envelope of a 2-parametric set of surfaces. The computation of the general envelope conditions between the valve tappet

Table 1: Symbols and their meanings.

Symbol	Meaning
s	shift parameter
t	rotation angle
$r = r(t)$	valve lift function
c	lobe curve
$\mathbf{c}(t)$	parameterization of a lobe curve
2β	valve opening angle
l	maximal lift
d	cam radius
$f = f(s, t)$	bivariate radius function
f_s, f_t	partial derivatives of the bivariate radius function $f = f(s, t)$
g	camshaft axis
$\mathbf{d} = \mathbf{d}(s, t)$	parameterization of the profile surface
Σ_0	camshaft mounting system
Σ_1	camshaft system
Σ_2	right cam system
$\bar{\Sigma}_2$	left cam system
Σ_3	valve system
$\{O_i, x_i, y_i, z_i\}$	coordinate frame in system Σ_i
P	reference point in the valve system Σ_3
Σ_j/Σ_i	relative motions
\mathbf{B}_{ij}	transformation matrix for the motion Σ_j/Σ_i
\mathbf{A}	rotation matrix
Φ	follower surface
\mathbf{n}	normal vector of the follower surface Φ
$\mathbf{v} = \mathbf{v}(u, v)$	parameterization of the follower surface Φ
$\mathbf{w} = \mathbf{w}(s, t, u, v)$	instances of the follower surface Φ w.r.t. the motion Σ_3/Σ_2
T, \bar{T}	contact points between follower surface and left/right cam
R_T	center circle radius of the torus
r_T	meridian radius of the torus
a	abbreviation for $-ff_s/R_T$ (computation of the angle u)
b	abbreviation for f_t/R_T (computation of the angle u)
k	unit circle (computation of the angle u)
h	hyperbola (computation of the angle u)

follower surface (in short: follower surface) and the cam surface turns out to be the trickiest part of the matter, addressed in Section 5. In Section 6 we specify the follower surface as part of a torus and compute the corresponding cam surface. In Section 7 we demonstrate the procedure in a concrete example. This gives us the opportunity to show the whole mechanism in action. In Section 8 our perceived contribution is emphasized and some practical considerations regarding implementation are mentioned. The reader will find in Table 1 all symbols with a short explanation of their meanings.

2. Input data

A *lift diagram* describes the valve lift as a function $r = r(t)$ of the rotation angle $t \in [0, 2\pi]$ (Figure 1, left). $r = r(t)$ can as well be interpreted as the polar coordinate equation of a closed curve, called *lobe curve*. Referring to the Cartesian coordinate frame $\{O; x, z\}$, shown in Figure 1, right, the parameterization of this lobe curve is given by

$$\mathbf{c}(t) = \begin{pmatrix} r(t) \cdot \sin(t) \\ -r(t) \cdot \cos(t) \end{pmatrix}. \quad (1)$$

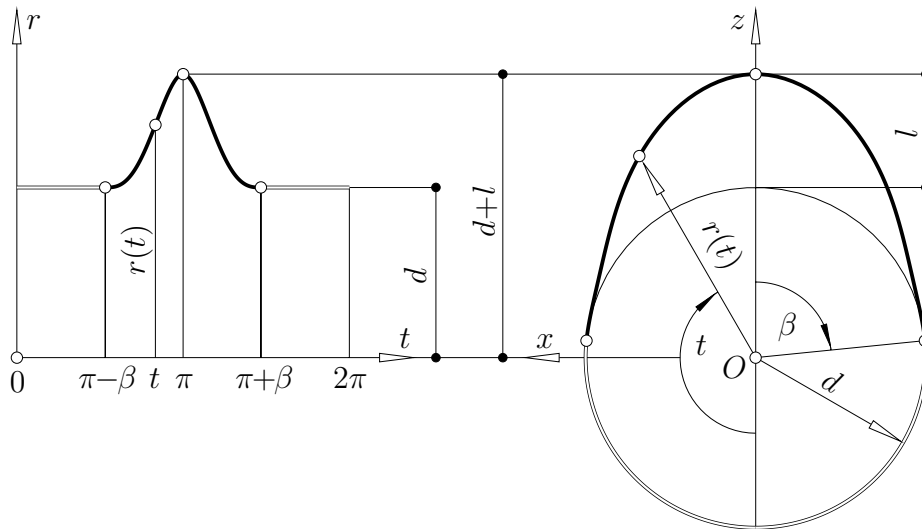


Figure 1: A lift diagram and its respective lobe curve.

We assume $r(2\pi - t) = r(t)$ which means that the lobe curve implies identical rise and fall profiles.¹ Clearly, there are two significant segments of this curve, controlled by the so-called *duration angle* 2β :

- For $t \in [\pi - \beta, \pi + \beta]$ the function $r = r(t)$ is non-constant whereas
- we have $r(t) = d = \text{const}$ while t runs in the two complementary intervals $[0, \pi - \beta]$ and $[\pi + \beta, 2\pi]$. Obviously, the remaining part of the lobe curve is a circular arc (double line in Figure 1, right). We call d the *cam radius*.

Let the maximal value $d + l$ of $r = r(t)$ be assumed at $t = \pi$:

$$r(\pi) = d + l.$$

¹The symmetry of the lobe curve is not a necessary condition for our proposed mechanism. This symmetry condition could as well be dropped.

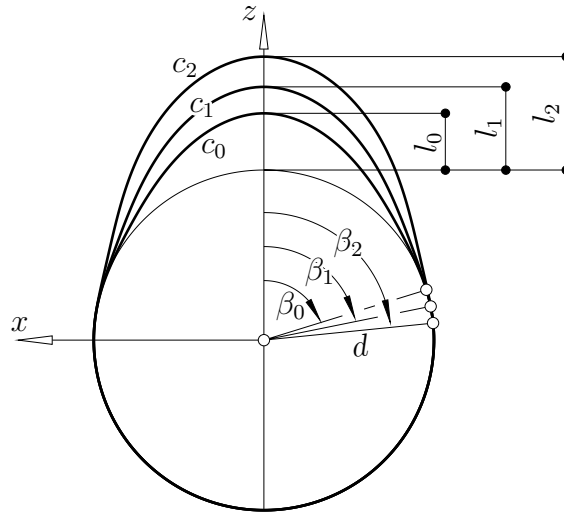


Figure 2: $k + 1$ different lobe curves are given ($k = 2$).

The dimension l is called the *maximal lift* of the lobe curve.

Now, let a sequence of — say $k + 1$ — lift diagrams for different engine states be given. For these diagrams we compute the corresponding $k + 1$ lobe curves c_0, \dots, c_k according to eq. (1). For every $i = 0, \dots, k$ the duration angle and maximal lift will be denoted by $2\beta_i$ and l_i , respectively (see Figure 2). We will use such a set of lobe curves as input data for our procedure.

Our aim is to construct a mechanism that is capable of moving the valve stem according to the given lobe curves c_i . Even more so, our solution should be able to continuously engage an infinity of lobe curves that can be computed by interpolation from the predefined curves c_i (see Section 3). For different engine states the appropriate valve lift schemes could be applied at any moment by the engine management controller.

3. The profile surface

Let $r_i = r_i(t)$ be the given lift diagrams and let c_i be the corresponding lobe curves, $i = 0, \dots, k$. Additionally we choose values s_i , $i = 0, \dots, k$ with $0 = s_0 < \dots < s_k = s_{max}$. By solving a standard interpolation problem (see, for instance, [5, p. 116–136]) for the input $s_i, r_i(t)$, $i = 0, \dots, k$, we obtain a bivariate function $f(s, t) > 0$, called *radius function* (see Figure 3) which satisfies

$$f(s_i, t) = r_i(t).$$

Based on this radius function we define a *profile surface* by means of the parameterization:

$$\mathbf{d}(s, t) = \begin{pmatrix} f(s, t) \cdot \sin t \\ s \\ -f(s, t) \cdot \cos t \end{pmatrix} \quad (2)$$

Obviously, the lobe curves c_i appear as t -parameter lines $s = s_i$ on this surface:

$$\mathbf{c}_i(t) := \mathbf{d}(s_i, t) = \begin{pmatrix} f(s_i, t) \cdot \sin(t) \\ s_i \\ -f(s_i, t) \cdot \cos(t) \end{pmatrix}.$$

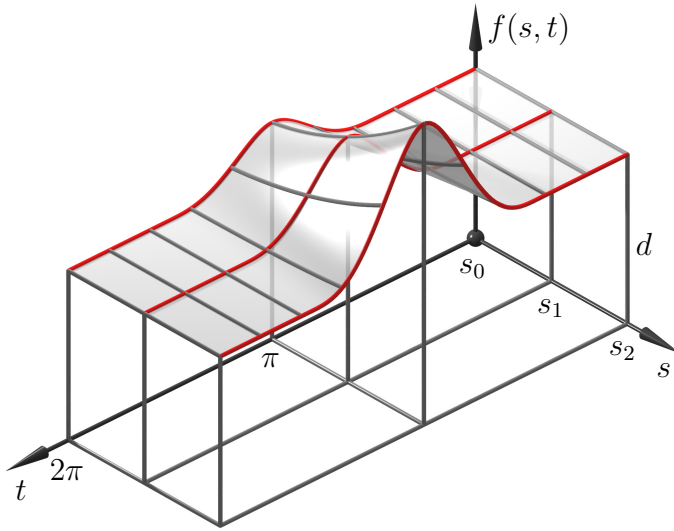


Figure 3: The bivariate radius function $r = f(s, t)$ interpolating the given lift diagrams $r = r_i(t)$ (red) at $s = s_i$; $i = 0, \dots, k$; in this figure we have $k = 2$.

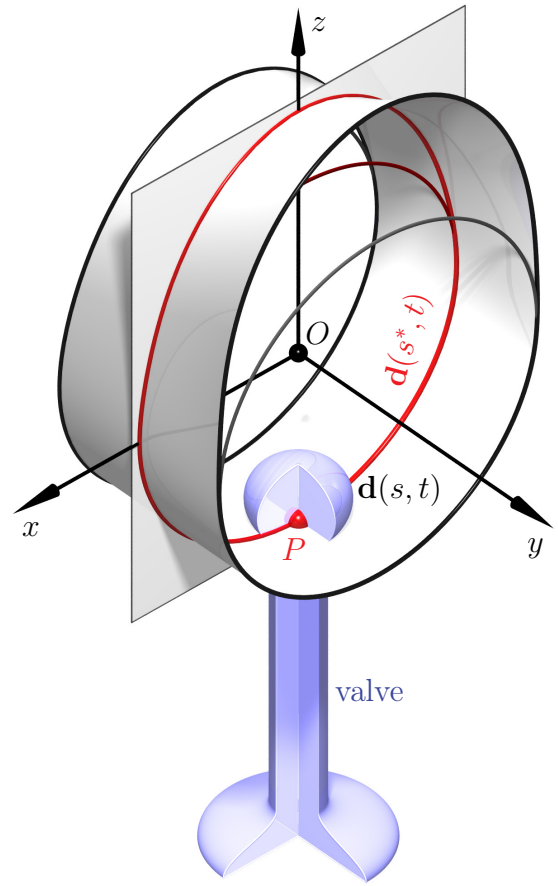


Figure 4: The virtual profile surface $\mathbf{d}(s, t)$ controlling the valve lift. The planar parameter line $\mathbf{d}(s^*, t)$ on that surface is the path of P w.r.t. a 1-parametric submotion of the 2-parametric valve-cam motion.

All other t -parameter lines $s = s^* = \text{const.}$ are planar curves as well, lying in planes $y = s^*$:

$$\mathbf{c}_{s^*}(t) := \mathbf{d}(s^*, t) = \begin{pmatrix} f(s^*, t) \cdot \sin(t) \\ s^* \\ -f(s^*, t) \cdot \cos(t) \end{pmatrix}. \quad (3)$$

We regard each of these curves $s = s^*$ as a potential lobe curve. Our intention is to construct the cam surface in a way that for any $s^* \in [0, s_{max}]$ the relative motion of the valve system w.r.t. the cam system drives a point P of the valve stem axis on the lobe curve $\mathbf{c}_{s^*}(t) = \mathbf{d}(s^*, t)$ (Figure 4).

In the parameter domain of t where all c_i are circular arcs of radius d (cam radius) we can achieve that the respective part of the profile surface is part of a right cylinder.

It is worth mentioning that the profile surface is different from the eventual cam shape of our variable cam mechanism (which will be constructed in Section 6). Even more so, the profile surface $\mathbf{d}(s, t)$ itself will not appear in substance anywhere in our cam mechanism. It is merely a virtual surface whose parallel cross sections $s = s^*$ represent the lobe curves

applied in different engine states. We imagine the virtual profile surface as being anchored in the cam system Σ_2 as to be explained in the following section.

4. The cam mechanism

The suggested cam mechanism consists of the following systems (Figure 5): the reference system Σ_0 (fixed system) containing the camshaft mounting, system Σ_1 accommodating the camshaft, Σ_3 containing the valve. The cam system Σ_2 will contain some hitherto unknown cam surface (on the right-hand side) and the aforementioned virtual profile surface which we introduced in Section 3. The cam is actually split into two symmetric parts which can be shifted synchronously along the cam axis. So the mechanism comprises one more system $\bar{\Sigma}_2$ containing the cam surface on the left-hand side. As this surface is symmetric to the right one we need not compute its shape separately. The design of the cam surface will be the central task of Section 6.

For the mathematical description we endow each system Σ_i with a local right-handed coordinate frame $\{O_i, x_i, y_i, z_i\}$. The frames for Σ_0 (camshaft mounting), Σ_1 (camshaft) and Σ_2 (cam) coincide in the initial position. The coordinate frame $\{O_3, x_3, y_3, z_3\}$ of Σ_3 (valve system) is centered in the aforementioned point P : $O_3 = P$. Its axes x_3, y_3, z_3 stay parallel to x_0, y_0, z_0 throughout the motion. The coordinate frames $\{O_2, x_2, y_2, z_2\}$ and $\{O_3, x_3, y_3, z_3\}$ can be seen in Figure 6 for a general state of the mechanism.

We now regard some relative motions Σ_i/Σ_j of the systems within our mechanism.

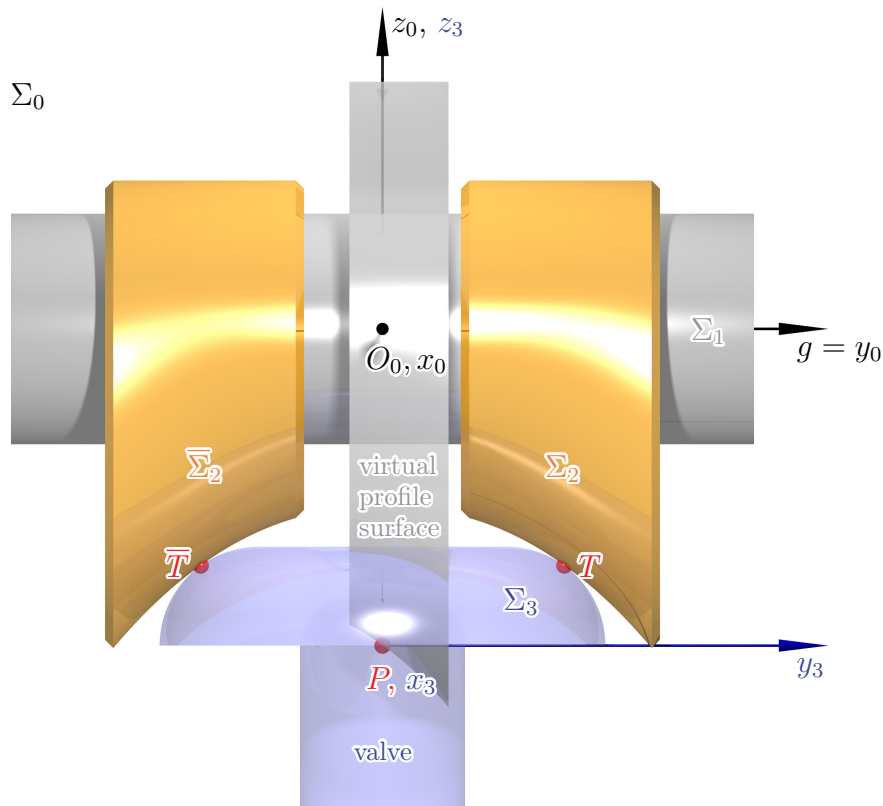


Figure 5: The systems of the valve control mechanism. The virtual profile surface anchored in system Σ_2 is the trajectory surface of the point P w.r.t. the 2-parameter motion Σ_3/Σ_2 (valve/cam); it is noted as mentioned before that this surface appears on no mechanical part.

- The motion Σ_1/Σ_0 of the camshaft Σ_1 with respect to the reference system Σ_0 is just a rotation about the camshaft axis g described by

$$\begin{pmatrix} 1 \\ x_0 \\ y_0 \\ z_0 \end{pmatrix} = \begin{pmatrix} 1 & 0 & 0 & 0 \\ 0 & \cos t & 0 & \sin t \\ 0 & 0 & 1 & 0 \\ 0 & -\sin t & 0 & \cos t \end{pmatrix} \cdot \begin{pmatrix} 1 \\ x_1 \\ y_1 \\ z_1 \end{pmatrix} =: \mathbf{B}_{01} \cdot \begin{pmatrix} 1 \\ x_1 \\ y_1 \\ z_1 \end{pmatrix}$$

in terms of the chosen coordinate frames in Σ_0 and Σ_1 .

- Σ_2/Σ_1 : The cam system Σ_2 is movable towards the system Σ_1 of the camshaft; it performs a pure translation in the direction of the camshaft axis g :

$$\begin{pmatrix} 1 \\ x_1 \\ y_1 \\ z_1 \end{pmatrix} = \begin{pmatrix} 1 & 0 & 0 & 0 \\ 0 & 1 & 0 & 0 \\ -s & 0 & 1 & 0 \\ 0 & 0 & 0 & 1 \end{pmatrix} \cdot \begin{pmatrix} 1 \\ x_2 \\ y_2 \\ z_2 \end{pmatrix} =: \mathbf{B}_{12} \cdot \begin{pmatrix} 1 \\ x_2 \\ y_2 \\ z_2 \end{pmatrix}.$$

The virtual profile surface is anchored in the cam system Σ_2 . A shift by the value $-s$ in y -direction brings the planar intersection $\mathbf{c}_s(t)$ of this surface in a position coincident with the plane $y_3 = 0$ in Σ_3 . This entails that — in this operating mode — the curve $\mathbf{c}_s(t)$ (see Section 3) on the profile surface represents the path of P w.r.t. the motion Σ_3/Σ_2 .

- The 2-parameter motion Σ_2/Σ_0 is the combination of the previous two relative motions. Thus, the respective transformation matrix \mathbf{B}_{02} can be built up as $\mathbf{B}_{02} = \mathbf{B}_{01} \cdot \mathbf{B}_{12}$:

$$\begin{pmatrix} 1 \\ x_0 \\ y_0 \\ z_0 \end{pmatrix} = \begin{pmatrix} 1 & 0 & 0 & 0 \\ 0 & \cos t & 0 & \sin t \\ -s & 0 & 1 & 0 \\ 0 & -\sin t & 0 & \cos t \end{pmatrix} \cdot \begin{pmatrix} 1 \\ x_2 \\ y_2 \\ z_2 \end{pmatrix} = \mathbf{B}_{02} \cdot \begin{pmatrix} 1 \\ x_2 \\ y_2 \\ z_2 \end{pmatrix}.$$

- Σ_3/Σ_0 : The valve Σ_3 translates with respect to Σ_0 along the valve stem axis $z_0 = z_3$ according to the bivariate radius function $f(s, t)$:

$$\begin{pmatrix} 1 \\ x_0 \\ y_0 \\ z_0 \end{pmatrix} = \begin{pmatrix} 1 & 0 & 0 & 0 \\ 0 & 1 & 0 & 0 \\ 0 & 0 & 1 & 0 \\ -f(s, t) & 0 & 0 & 1 \end{pmatrix} \cdot \begin{pmatrix} 1 \\ x_3 \\ y_3 \\ z_3 \end{pmatrix} =: \mathbf{B}_{03} \cdot \begin{pmatrix} 1 \\ x_3 \\ y_3 \\ z_3 \end{pmatrix}.$$

- Let us now focus on the relative motion Σ_3/Σ_2 of Σ_3 (valve) w.r.t. Σ_2 (cam). The

transformation matrix \mathbf{B}_{23} of this motion can be computed as $\mathbf{B}_{23} = \mathbf{B}_{02}^{-1} \cdot \mathbf{B}_{03}$:

$$\begin{aligned}
\begin{pmatrix} 1 \\ x_2 \\ y_2 \\ z_2 \end{pmatrix} &= \mathbf{B}_{02}^{-1} \cdot \mathbf{B}_{03} \cdot \begin{pmatrix} 1 \\ x_3 \\ y_3 \\ z_3 \end{pmatrix} \\
&= \begin{pmatrix} 1 & 0 & 0 & 0 \\ 0 & \cos t & 0 & -\sin t \\ s & 0 & 1 & 0 \\ 0 & \sin t & 0 & \cos t \end{pmatrix} \cdot \begin{pmatrix} 1 & 0 & 0 & 0 \\ 0 & 1 & 0 & 0 \\ 0 & 0 & 1 & 0 \\ -f(s,t) & 0 & 0 & 1 \end{pmatrix} \cdot \begin{pmatrix} 1 \\ x_3 \\ y_3 \\ z_3 \end{pmatrix} \\
&= \begin{pmatrix} 1 & 0 & 0 & 0 \\ f(s,t) \cdot \sin t & \cos t & 0 & -\sin t \\ s & 0 & 1 & 0 \\ -f(s,t) \cdot \cos t & \sin t & 0 & \cos t \end{pmatrix} \cdot \begin{pmatrix} 1 \\ x_3 \\ y_3 \\ z_3 \end{pmatrix}. \tag{4}
\end{aligned}$$

5. Envelope considerations

In fact, the valve stem is not a single rod which is pushed by the cam. It rather carries the so-called valve spring retainer which keeps the valve spring in place. Its follower surface Φ can be a flat disk or any other shape for whatever reason. The important thing is that the cam surface is the envelope surface of the follower surface Φ w.r.t. the 2-parametric motion Σ_3/Σ_2 (valve system vs. cam system), see Figure 6. This enables us to compute the cam surface shape; cf. [1, pp. 355]:

Equation (4) can also be written as

$$\begin{pmatrix} x_2 \\ y_2 \\ z_2 \end{pmatrix} = \underbrace{\begin{pmatrix} f(s,t) \cdot \sin t \\ s \\ -f(s,t) \cdot \cos t \end{pmatrix}}_{=: \mathbf{d}(s,t)} + \underbrace{\begin{pmatrix} \cos t & 0 & -\sin t \\ 0 & 1 & 0 \\ \sin t & 0 & \cos t \end{pmatrix}}_{=: \mathbf{A}(t)} \cdot \begin{pmatrix} x_3 \\ y_3 \\ z_3 \end{pmatrix}. \tag{5}$$

Note that $\mathbf{A}(t)$ is a proper orthogonal matrix (rotation matrix), i.e., $\mathbf{A}^{-1} = \mathbf{A}^\top$, $\det \mathbf{A} = 1$.

Moreover, we know that the path of $P = O_3$ is parameterized by the translational part $\mathbf{d}(s,t)$ of the motion Σ_3/Σ_2 (cf. (2)).

Let the follower surface Φ be given by some parameterization

$$\mathbf{v}(u,v) = \begin{pmatrix} x_3(u,v) \\ y_3(u,v) \\ z_3(u,v) \end{pmatrix} =: \begin{pmatrix} x(u,v) \\ y(u,v) \\ z(u,v) \end{pmatrix}. \tag{6}$$

If we subject this surface to the motion Σ_3/Σ_2 (eq. (5)) we obtain

$$\begin{aligned}
\mathbf{w}(s,t,u,v) &= \mathbf{d}(s,t) + \mathbf{A}(t) \cdot \mathbf{v}(u,v) \\
&= \mathbf{d}(s,t) + \mathbf{A}(t) \cdot \begin{pmatrix} x(u,v) \\ y(u,v) \\ z(u,v) \end{pmatrix}. \tag{7}
\end{aligned}$$

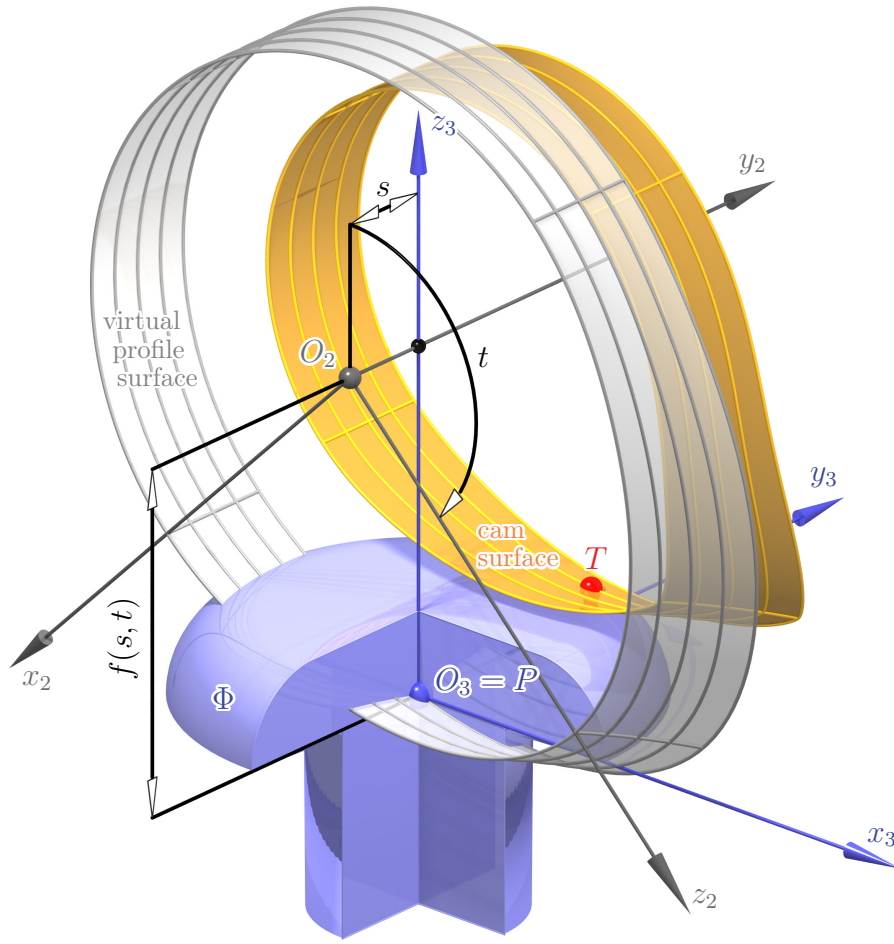


Figure 6: While the point P of the valve system (blue) moves on the virtual profile surface the cam surface (yellow) is generated as the envelope of the follower Φ on the valve stem. The instantaneous contact point of the cam surface and Φ is T .

For given values s, t equation (7) represents the instance of Φ to these motion parameters s, t . We aim at computing the envelope surface (cam surface) of all these instances. Every such instance is tangent to the envelope surface in a particular contact point T , i.e., the two surfaces have a common tangent plane τ_1 in that point T . If Ψ is the trajectory surface of T w.r.t. the motion Σ_3/Σ_2 and τ_2 is the tangent plane of Ψ in T , then τ_2 must be identical to τ_1 which delivers the envelope conditions: As τ_1 has the normal vector

$$\mathbf{w}_u \times \mathbf{w}_v$$

and τ_2 is spanned by the two vectors²

$$\frac{\partial \mathbf{w}}{\partial s} = \mathbf{d}_s + \mathbf{A}_s \mathbf{v}, \quad \frac{\partial \mathbf{w}}{\partial t} = \mathbf{d}_t + \mathbf{A}_t \mathbf{v}$$

these envelope conditions become³

$$\begin{aligned} \langle \mathbf{d}_s + \mathbf{A}_s \mathbf{v}, \mathbf{w}_u \times \mathbf{w}_v \rangle &= 0, \\ \langle \mathbf{d}_t + \mathbf{A}_t \mathbf{v}, \mathbf{w}_u \times \mathbf{w}_v \rangle &= 0. \end{aligned} \tag{8}$$

²The subscripts in these and the following equations stand for differentiation w.r.t. the indicated parameters.

³ $\langle \cdot, \cdot \rangle$ denotes the standard scalar product of two vectors.

From (7) it is obvious that $\mathbf{w}_u = \mathbf{A} \cdot \mathbf{v}_u$, $\mathbf{w}_v = \mathbf{A} \cdot \mathbf{v}_v$ and as \mathbf{A} is orthogonal $\mathbf{w}_u \times \mathbf{w}_v = (\mathbf{A} \cdot \mathbf{v}_u) \times (\mathbf{A} \cdot \mathbf{v}_v) = \mathbf{A} \cdot (\mathbf{v}_u \times \mathbf{v}_v)$. Thus (8) can be written as

$$\begin{aligned} \langle \mathbf{d}_s + \mathbf{A}_s \mathbf{v}, \mathbf{A}(\mathbf{v}_u \times \mathbf{v}_v) \rangle &= 0, \\ \langle \mathbf{d}_t + \mathbf{A}_t \mathbf{v}, \mathbf{A}(\mathbf{v}_u \times \mathbf{v}_v) \rangle &= 0. \end{aligned} \quad (9)$$

or as

$$\begin{aligned} \langle \mathbf{A}^\top \mathbf{d}_s + \mathbf{A}^\top \mathbf{A}_s \mathbf{v}, \mathbf{A}^\top \mathbf{A}(\mathbf{v}_u \times \mathbf{v}_v) \rangle &= 0, \\ \langle \mathbf{A}^\top \mathbf{d}_t + \mathbf{A}^\top \mathbf{A}_t \mathbf{v}, \mathbf{A}^\top \mathbf{A}(\mathbf{v}_u \times \mathbf{v}_v) \rangle &= 0. \end{aligned} \quad (10)$$

Moreover we have:

- \mathbf{A}_s is the 3×3 zero matrix as \mathbf{A} is a function of t only.
- $\mathbf{A}^\top \mathbf{A}$ is the 3×3 identity matrix as \mathbf{A} is orthogonal.
- $\mathbf{A}^\top \mathbf{A}_t$ yields the simple skew symmetric matrix

$$\mathbf{A}^\top \mathbf{A}_t = \begin{pmatrix} 0 & 0 & -1 \\ 0 & 0 & 0 \\ 1 & 0 & 0 \end{pmatrix} =: \mathbf{W}.$$

With that in mind, the conditions (10) reduce to

$$\begin{aligned} \langle \mathbf{A}^\top \mathbf{d}_s, \mathbf{v}_u \times \mathbf{v}_v \rangle &= 0, \\ \langle \mathbf{A}^\top \mathbf{d}_t + \mathbf{W} \mathbf{v}, \mathbf{v}_u \times \mathbf{v}_v \rangle &= 0. \end{aligned}$$

Remember that $\mathbf{v}_u \times \mathbf{v}_v$ is the normal vector

$$\mathbf{n} = \mathbf{v}_u \times \mathbf{v}_v =: \begin{pmatrix} n_1 \\ n_2 \\ n_3 \end{pmatrix}$$

of the follower surface Φ . Using (6) we obtain

$$\begin{aligned} \left\langle \begin{pmatrix} 0 \\ 1 \\ -f_s \end{pmatrix}, \begin{pmatrix} n_1 \\ n_2 \\ n_3 \end{pmatrix} \right\rangle &= 0, \\ \left\langle \begin{pmatrix} f \\ 0 \\ -f_t \end{pmatrix} + \begin{pmatrix} 0 & 0 & -1 \\ 0 & 0 & 0 \\ 1 & 0 & 0 \end{pmatrix} \begin{pmatrix} x \\ y \\ z \end{pmatrix}, \begin{pmatrix} n_1 \\ n_2 \\ n_3 \end{pmatrix} \right\rangle &= 0, \end{aligned}$$

and finally arrive at the envelope conditions

$$\begin{aligned} n_2 - f_s n_3 &= 0, \\ (f - z)n_1 + (-f_t + x)n_3 &= 0. \end{aligned} \quad (11)$$

6. Shaping the cam

As derived in Section 5 the envelope of the follower surface Φ w.r.t. the motion Σ_3/Σ_2 (valve system vs. cam system) is the cam surface. Once a particular follower surface has been chosen by means of its parameterization (6), a parameterization of the cam surface in s, t can be determined

- by solving the two envelope conditions (11) for u and v :

$$u = u(s, t), \quad v = v(s, t)$$

- and, in a second step, by substituting this solution into (7).

The first idea for the shape of Φ will, most probably, be that of a hemisphere. For technical reasons, however, this option is not viable.⁴

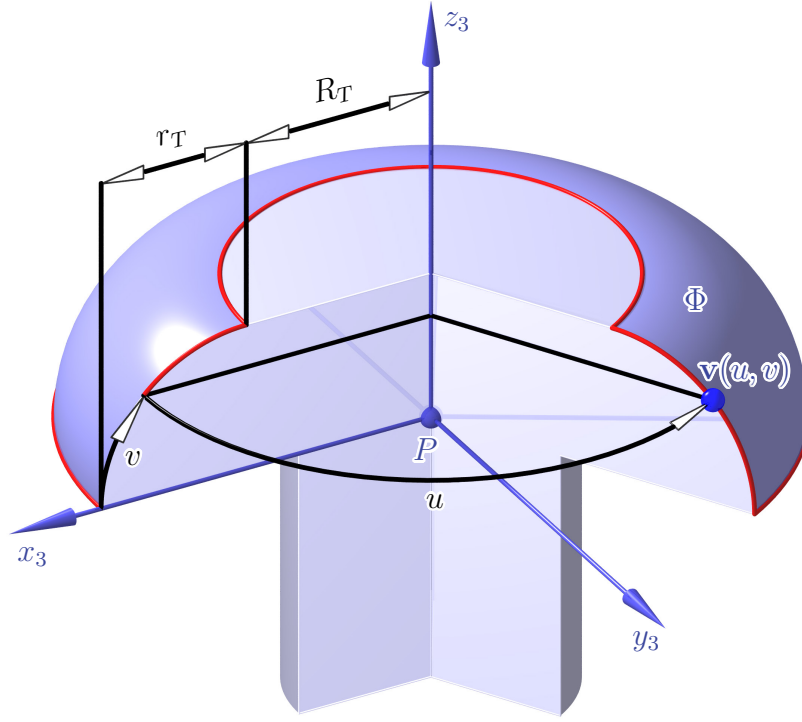


Figure 7: Toroidal follower surface Φ .

Let us choose a torus with axis z_3 and center $O_3 = P$ as the surface Φ ; then

$$\mathbf{v}(u, v) = \begin{pmatrix} x(u, v) \\ y(u, v) \\ z(u, v) \end{pmatrix} = \begin{pmatrix} \cos u \cdot (R_T + r_T \cos v) \\ \sin u \cdot (R_T + r_T \cos v) \\ r_T \sin v \end{pmatrix} \quad (12)$$

is a parameterization of this surface (see Figure 7). R_T is the torus center circle radius, while r_T is its meridian radius. Obviously, only the upper right quarter of the torus can contain potential contact points with the right cam surface. This torus region is obtained by (12) for $(u, v) \in [0, \pi] \times [0, \frac{\pi}{2}]$.

A normal vector of the torus for the parameter values u, v can be computed via

$$\mathbf{n}(u, v) = \begin{pmatrix} n_1(u, v) \\ n_2(u, v) \\ n_3(u, v) \end{pmatrix} = \begin{pmatrix} \cos u \cos v \\ \sin u \cos v \\ \sin v \end{pmatrix}. \quad (13)$$

⁴Using a hemisphere as the follower surface would certainly simplify the computation of the envelope surface (cam surface). However, this would imply that the gap between the two halves Σ_2 and $\bar{\Sigma}_2$ of the cam vanishes. In this case we would not be able to shift Σ_2 and $\bar{\Sigma}_2$ towards each other anymore.

Substitution of (12) and (13) into (11) yields

$$\sin u \cos v - f_s \sin v = 0, \quad (14)$$

$$f \cos u \cos v + (-f_t + R_T \cos u) \sin v = 0 \quad (15)$$

as envelope conditions for a torus-shaped follower surface. The following theorem will guarantee that under certain assumptions these envelope conditions can always be solved uniquely.

Theorem 1. *Let the following two preconditions be fulfilled:*

$$f_s \geq 0, \quad (16)$$

$$\text{if } f_s = 0 \text{ then } |f_t| < R_T. \quad (17)$$

Then the envelope conditions (14), (15) have a unique solution u, v in $[0, \pi] \times [0, \frac{\pi}{2}]$ for every input triple $f > 0, f_s, f_t$.

Proof. We elaborate on the statement by considering three different cases.

Case 1: $f_t = 0$.

Then (15) reads as

$$\cos u \cdot (f \cos v + R_T \sin v) = 0. \quad (18)$$

Due to $f, R_T > 0$ we have $f \cos v + R_T \sin v \neq 0$ for v in $[0, \frac{\pi}{2}]$. This implies $\cos u = 0$, so $u = \frac{\pi}{2}$ is the only possible solution in $[0, \pi]$. So, the first envelope condition (14) is

$$\cos v - f_s \sin v = 0. \quad (19)$$

Mind that $f_s \geq 0$, so we get a unique solution $v \in [0, \frac{\pi}{2}]$.

Case 2: $f_t \neq 0, f_s = 0$.

The first envelope condition (14) simplifies to

$$\sin u \cdot \cos v = 0. \quad (20)$$

The option $\sin u = 0$, i.e., $u = 0$ or $u = \pi$ and (15) yield

$$\tan v = -\frac{f}{R_T \mp f_t}.$$

Due to precondition (17) the right hand side of this equation is negative which means that this equation delivers no solution for v in $[0, \frac{\pi}{2}]$. Thus, the only option in case 2 is $\cos v = 0$ which means $v = \frac{\pi}{2}$. Then the envelope condition (15) reads as

$$\cos u = \frac{f_t}{R_T}$$

which provides a unique value $u \in [0, \pi]$ according to (17).

Case 3: $f_t \neq 0, f_s > 0$.

The envelope conditions (14), (15) are two linear homogeneous equations in $\cos v$ and $\sin v$; they will only deliver non-trivial solutions if the coefficient matrix is singular:

$$R_T \cos u \sin u + f f_s \cos u - f_t \sin u = 0. \quad (21)$$

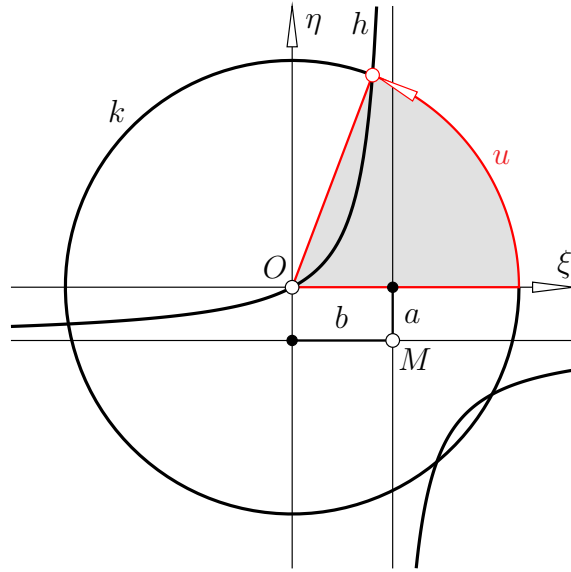


Figure 8: In the general case, finding the angle u to a given pair (s, t) amounts to intersecting a rectangular hyperbola h with the unit circle k .

This equation is free from the parameter v . Together with (14) it controls the envelope surface. The abbreviations $a := -\frac{ff_s}{R_T}$, $b := \frac{f_t}{R_T}$ finally convey our two envelope conditions

$$\sin u \cos v - f_s \sin v = 0, \quad (22)$$

$$\cos u \sin u - a \cos u - b \sin u = 0, \quad (23)$$

which we have to solve for u, v . In order to reveal the nature of condition (23) we put $\xi := \cos u$ and $\eta := \sin u$. This way we have parameterized the unit circle k in the $\xi\eta$ -plane. Condition (23) now reads as

$$\xi\eta - a\xi - b\eta = 0. \quad (24)$$

Owing to $a, b \neq 0$ this curve can easily be identified as a hyperbola h in the $\xi\eta$ -plane (see Figure 8) with the following properties:

- The center of h is (b, a) ; note that, according to (16) we have $a = -\frac{ff_s}{R_T} < 0$ which means that this center lies below the ξ -axis.
- h contains the origin $O(0, 0)$.
- The asymptotes of h are parallel to the coordinate axes.

We have to intersect this hyperbola h with the *northern part* ($u \in [0, \pi]$) of the unit circle k . Due to the aforementioned properties of the hyperbola h it is obvious that there exists a unique point of intersection of that kind. Using the Newton method with some appropriate starting value u_0 we easily get this intersection point with sufficient numerical accuracy. This conveys the respective value u .

Subsequently, we obtain from (22)

$$\tan v = \frac{\sin u}{f_s}$$

which delivers a unique solution v in $[0, \frac{\pi}{2}]$ as $\sin u > 0$ and $f_s > 0$. \square

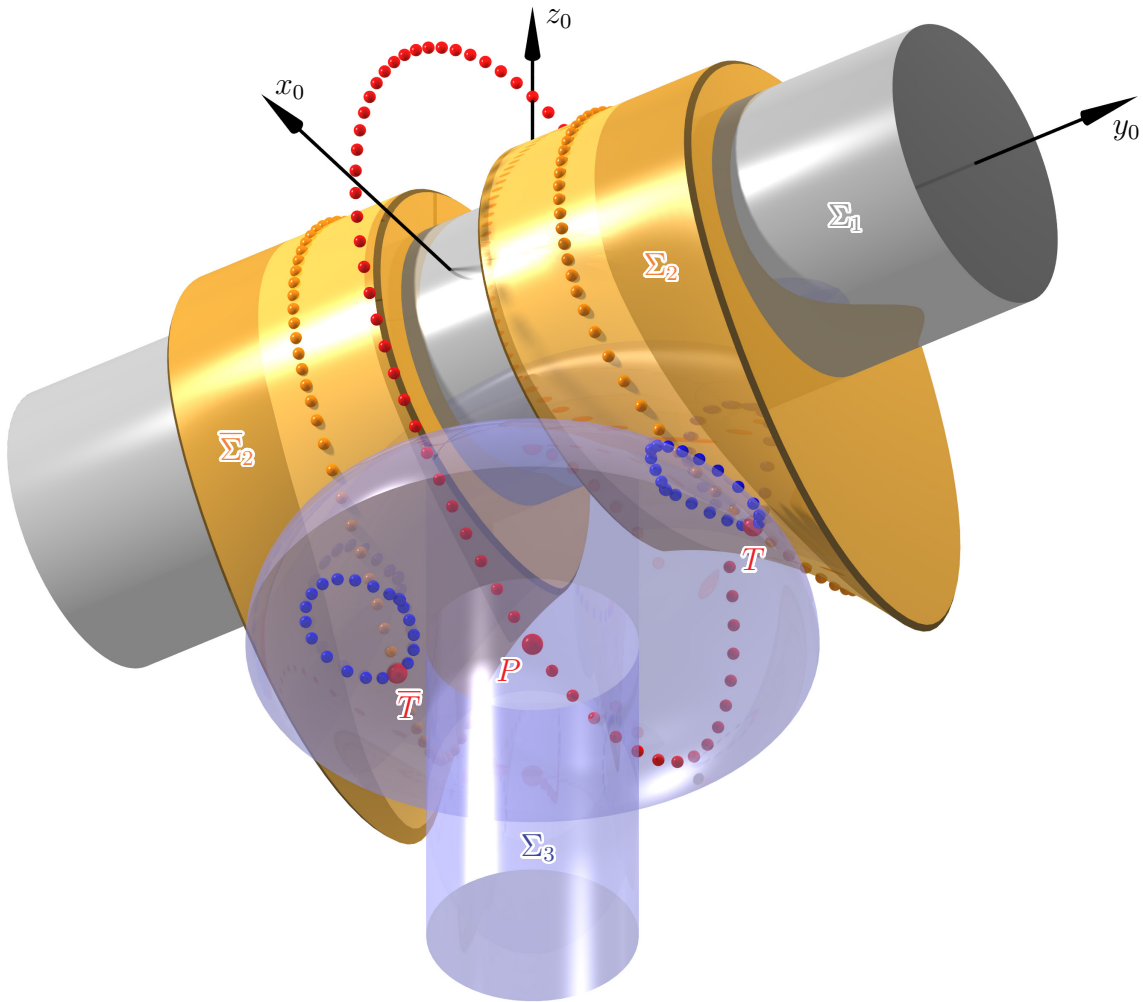


Figure 9: The variable valve control mechanism.

Remark. Areas of the profile surface (2) that are parts of a cylinder of revolution will always yield $f_s = f_t = 0$. Case 1 from above implies $u = v = \frac{\pi}{2}$. Inserting into (12) and transforming the result into system Σ_2 via (5) we arrive at a cylindric part of the envelope surface: The respective area of our cam surface is part of a cylinder of revolution.

7. An example

In the previous sections we have described the tools for fully variable valve control. We now apply them to a particular example.

- We start with a set of three given valve lift diagrams $r_i(t)$ for $i = 0, 1, 2$ and their respective lobe curves $\mathbf{c}_i(t)$. We have $d = 30.0$, the maximal lifts of the three predefined profiles $\mathbf{c}_i(t)$ are set to $l_0 = 6.0$, $l_1 = 10.0$, $l_2 = 16.0$. For the valve duration angles $2\beta_i$ we choose $\beta_0 = 1.42 \text{ rad} \hat{=} 81.40^\circ$, $\beta_1 = 1.57 \text{ rad} \hat{=} 90^\circ$, $\beta_2 = 1.72 \text{ rad} \hat{=} 98.6^\circ$. As for the width dimensions we use $s_0 = 0$, $s_1 = 6.0$, $s_2 = s_{max} = 12.0$. The torus Φ is determined by the radii $R_T = 15.0$ and $r_T = 12.0$.
- For the interpolation to create the radius function $f(s, t)$ we apply the univariate Lagrange method of degree 2 (see [5, p. 119–122]) in the parameter s for each constant

value t . The emerging parameterization (2) represents the virtual profile surface $\mathbf{d}(s, t)$.

- The envelope conditions (14), (15) for the torus-shaped follower surface enable us to determine the cam surface just as demonstrated in Section 6.
- For any chosen value of the parameter s the point of contact T on the torus Φ runs on a contact curve (Figure 9, blue dotted curve) while the camshaft performs a full round. The respective contact point on the cam surface runs through the corresponding cam contact curve (Figure 9, yellow dotted curve).
- Due to the symmetric layout of the cam mechanism we also have a symmetric copy of the contact curve on the torus Φ . In the points of that curve the left hand side cam in $\bar{\Sigma}_2$ is tangent to the torus surface. It belongs to the respective contact curve on the left-hand side cam.
- The red dotted curve in Figure 9 is the path of point P w.r.t. the motion Σ_3/Σ_2 (motion valve/cam). This curve is one parameter line $s = s^*$ on the virtual profile surface $\mathbf{d}(s, t)$ (see (2)) for some fixed s^* .

With this in mind it is easy to create a video showing the whole mechanism in action. Figure 9 is actually a freeze image from such a video.

The two-part cam consists of Σ_2 and $\bar{\Sigma}_2$ (yellow). Modifying the parameter s shifts these two parts symmetrically along the camshaft axis y such that the gap between them shrinks or expands. At any moment the follower surface is tangent to each of the two symmetric cam surfaces. The areas on the cam surfaces where the contact between the follower surface and the cam bodies occurs are rendered brighter in Figure 9.

8. Conclusions

This paper addresses a particular approach to fully variable valve control. It is a mechanical solution attained by geometrical considerations. The core part of this contribution is the design of the cam itself which is divided in two. Focussing on geometric issues we did not address details peculiar to material properties, contact stress or lubrication. These are left to the expertise of the engineer. The production of the cam as designed in this paper is more challenging than that of an ordinary cam for non-variable valve control; the latter is basically cylindrical with the profile of a planar lobe curve.

Manufacturing each part of our two-piece cam could be a rewarding application of 3D-printing of components if this technology becomes capable of providing the necessary strength and dimensional precision required. The material has to cope with the two-point contact between the follower surface and the two halves of the cam.

The benefits of our proposal include the clean and straightforward mechanical layout and full control of valve timing, valve lift and the valve opening angle.

References

- [1] O. BOTTEMA, B. ROTH: *Theoretical Kinematics*. Dover Publications, 1990.
- [2] T. DRESNER, P. BARKAN: *A review and classification of variable valve timing mechanisms*. SAE Technical Paper 890674, 1989.
- [3] H. EICHLSEDER, M. KLÜTING, W.F. PIOCK: *Grundlagen und Theorie des Ottomotors — Der Fahrzeugantrieb*. Springer, Wien 2008.

- [4] C. GRAY: *A review of variable engine valve timing*. SAE Transactions **97**, 631–641 (1989).
- [5] M. HIRZ, W. DIETRICH, A. GFRERRER, J. LANG: *Integrated Computer-Aided Design in Automotive Development*. Springer, Heidelberg 2013.
- [6] M. KLÜTING, C. LANDERL: *Der neue Sechszylinder-Ottomotor von BMW, Teil 1: Konzept und konstruktive Merkmale*. MTZ **65**, 868–880 (2004).
- [7] T. KONNO: *Valve operating apparatus for an internal combustion engine*. US Patent Nr. 4848285, 1989.
- [8] J. LIEBL, M. KLÜTING, J. POGGEL, S. MISSY: *Der neue BMW Vierzylinder-Ottomotor mit Valvetronic, Teil 2: Thermodynamik und funktionale Eigenschaften*. MTZ **62**, 570–579 (2001).

Received November 17, 2017; final form February 21, 2018